JACS
JOURNAL OF THE AMERICAN CHEMICAL SOCIETY

Communication

pubs.acs.org/JACS

Long-Lived Nuclear Spin States in Methyl Groups and Quantum-Rotor-Induced Polarization

Benno Meier, Jean-Nicolas Dumez, Gabriele Stevanato, Joseph T. Hill-Cousins, Soumya Singha Roy, Pär Håkansson, Salvatore Mamone, Richard C. D. Brown, Giuseppe Pileio, and Malcolm H. Levitt*

School of Chemistry, University of Southampton, SO17 1BJ Southampton, U.K.

Supporting Information

ABSTRACT: Substances containing rapidly rotating methyl groups may exhibit long-lived states (LLSs) in solution, with relaxation times substantially longer than the conventional spin-lattice relaxation time T_1. The states become long-lived through rapid internal rotation of the CH_3 group, which imposes an approximate symmetry on the fluctuating nuclear spin interactions. In the case of very low CH_3 rotational barriers, a hyperpolarized LLS is populated by thermal equilibration at liquid helium temperature. Following dissolution, cross-relaxation of the hyperpolarized LLS, induced by heteronuclear dipolar couplings, generates strongly enhanced antiphase NMR signals. This mechanism explains the NMR signal enhancements observed for ^{13}C-γ-picoline (Icker, M.; Berger, S. *J. Magn. Reson.* **2012**, *219*, 1−3).

Groups of coupled nuclei may support long-lived states (LLSs) with spin memory lifetimes exceeding the conventional relaxation time T_1 by more than an order of magnitude.[1] Storing nuclear spin hyperpolarization in such states may extend the applicability of techniques such as dissolution dynamic nuclear polarization (DNP),[2] a method capable of enhancing NMR signals by more than 4 orders of magnitude that has already been used to characterize human cancer.[3]

When only two spins-$^1/_2$ are involved, the nuclear spin states may form a singlet state, which is antisymmetric with respect to spin exchange, and three triplet states, which are symmetric with respect to spin exchange. The imbalance between the singlet population and the mean triplet population is conserved under many major relaxation mechanisms, including the intramolecular dipole-dipole mechanism. The singlet-triplet population imbalance comprises the LLS, and in this case is called singlet order.[1f]

The situation with more than two spins-$^1/_2$ is more complex. LLSs, which are immune to intramolecular dipole-dipole relaxation, only exist in rigid molecules if the geometrical arrangement of nuclei possesses an inversion center.[1g,h] Since three proton nuclei of a methyl group form an equilateral triangle, which does not possess an inversion center, a LLS with a lifetime significantly longer than T_1 is not anticipated. Nevertheless, we now demonstrate the existence of such a state. It is long-lived because the CH_3 group rotates rapidly with respect to the rest of the molecule at room temperature. As discussed below, a CH_3 group supports long-lived spin order only if the correlation time τ_R associated with the CH_3 rotational diffusion about the ternary axis is much shorter than the correlation time τ_C for the overall molecular tumbling (Figure 1). Furthermore, the LLS may act as a repository for nuclear hyperpolarization. The hyperpolarized LLS does not lead directly to an enhanced NMR signal but may be observed indirectly through cross-relaxation effects which couple the nonmagnetic long-lived spin order to observable magnetization.

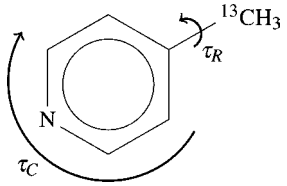

Figure 1. Structure of ^{13}C-γ-picoline. Relaxation of the LLS is controlled by correlation times τ_R and τ_C, which characterize the rotational diffusion of the CH_3 group and the entire molecule, respectively.

Effects of this kind are observed in the rapidly rotating CH_3 group of ^{13}C-γ-picoline (4-[^{13}C-methyl]pyridine, see Figure 1). Unusual NMR signal enhancements have been observed on this material when it was equilibrated at liquid helium temperature and then dissolved with a warm solvent.[4] These effects have correctly been attributed to the very low barrier for CH_3 rotation in γ-picoline, which leads to a large quantum rotor splitting and associated phenomena such as the Haupt effect.[5] For γ-picoline, the detailed mechanism of the hyperpolarization effects in solution, and especially the role of the ^{13}C nucleus, is so far unknown. We now show that the solution-state polarization effects in ^{13}C-γ-picoline, described by Icker and Berger,[4] may be explained by a quantum-rotor-induced population imbalance between states belonging to different irreducible representations of the spin permutation group, where the population imbalance occurs at temperatures below the rotor splitting. Upon dissolution the imbalance persists and equilibration occurs only slowly via cross-relaxation processes which give rise to enhanced NMR signals.

The methyl region of the ^{13}C and ^{1}H NMR spectra for γ-picoline are shown in Figure 2. All spectra were obtained without proton decoupling. Figure 2a shows the ^{13}C spectrum of a thermal equilibrium sample, displaying the well-known 1:3:3:1 quartet pattern with a heteronuclear J-coupling, J_{CH} = 127 Hz.

The spectrum in Figure 2b was obtained by equilibrating ^{13}C-γ-picoline for ∼2 h at 4 K in a DNP polarizer *without* switching on the microwave, rapidly dissolving it in degassed chloroform using

Received: October 10, 2013
Published: November 20, 2013

   dx.doi.org/10.1021/ja410432f | *J. Am. Chem. Soc.* 2013, 135, 18746−18749

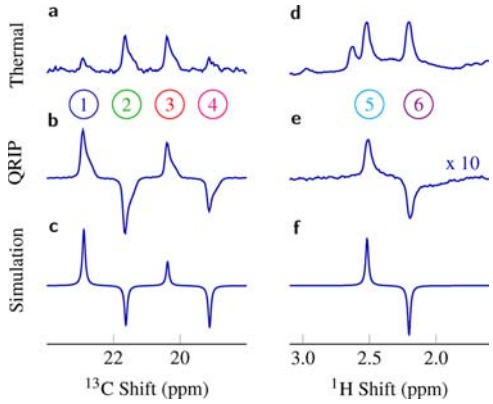

Figure 2. (a) Experimental ^{13}C spectrum after thermal equilibration in the magnetic field [90° flip angle, 32 transients added], (b) enhanced spectrum after dissolution [~10° flip angle], and (c) numerical simulation. (d) Experimental ^{1}H spectrum after thermal equilibration in the magnetic field [90° flip angle, 32 transients added], (e) enhanced spectrum after dissolution [~5° flip angle], and (f) simulated spectrum. All spectra were obtained on a solution of ^{13}C-γ-picoline in degassed $CHCl_3$ without proton decoupling in a magnetic field of 9.4 T. For experimental details see the SI. Simulations included dipole-dipole relaxation, CSA relaxation (with $\sigma^{C}_{zz} - \sigma^{C}_{iso} = 24$ ppm and $\sigma^{H}_{zz} - \sigma^{H}_{iso} = 5$ ppm), and random-field relaxation [$(\gamma_C \overline{B}^{C}_{rand})^2 \tau_{rand} = 44 \times 10^{-3}$ s^{-1} and $(\gamma_H \overline{B}^{H}_{rand})^2 \tau_{rand} = 24 \times 10^{-3}$ s^{-1}]. The correlation times were $\tau_C = 5$ ps and $\tau_R = 0.6$ ps. An initial relaxation delay of 15 s with no CSA relaxation was included to account for the delay before sample injection.

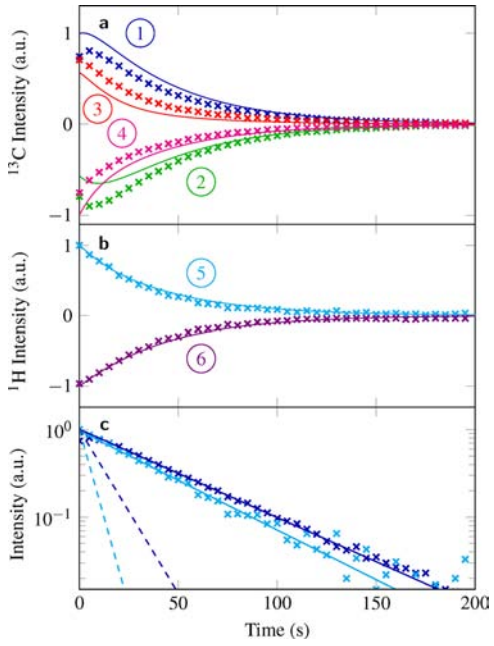

Figure 3. (a) Amplitudes of the ^{13}C peaks as a function of time, in an experiment in which a series of 10° pulses, separated by 5s, is applied after dissolution and transfer to the high-field magnet. Solid lines are numerical simulations of the peak amplitudes, scaled vertically for best fit to experimental data. (b) Same as in (a) for the ^{1}H peaks, obtained using 5° pulses. (c) Decay of two representative signals (1 and 5 in Figure 2) plotted on a logarithmic scale. The solid lines are obtained by fitting a monoexponential decay to the data at times ≥20 s. The fit procedure yields constants of 43.1 ± 0.4 s and 38 ± 2 s for ^{13}C (blue) and ^{1}H (cyan), respectively. Experimental T_1 decays of the ^{13}C (blue) and ^{1}H (cyan) magnetization are shown by dashed straight lines, for comparison. The simulation parameters are as in Figure 2.

dissolution-DNP equipment,[6] transferring it to a 9.4 T magnet, waiting another 10 s, and applying a ^{13}C pulse with a flip angle of ~10°. As in the original Icker–Berger experiment,[4a] an enhanced ^{13}C multiplet is observed, with irregular peak amplitudes of alternating sign. The magnitude of the enhancement with respect to the thermal signal at 9.4 T varies from peak to peak and is in the range 240–700 (taking the 10° flip angle into account). The significantly larger enhancement compared to ref 4a is attributed to the use of a fast dissolution apparatus.

Figure 2d,e shows the analogous data for the CH_3 protons. The hyperpolarized ^{1}H spectrum in Figure 2e was obtained using a 5° flip angle 10 s after injection of the sample into the magnet. The measured enhancement for the two peaks is ~±30.

Figure 3a shows experimental data for the ^{13}C peak amplitudes as a function of time (crosses). The four data sets were obtained by applying ^{13}C pulses of ~10° flip angle, separated by 5 s. After a short buildup period, the spectral intensities decay approximately exponentially with respect to time, with a time constant $T_{LLS} = 43 \pm 1$ s. Figure 3b shows analogous data for the ^{1}H magnetization obtained in a second experiment using ~5° flip angle pulses every 5 s. The time constant of the decay is found to be 38 s, i.e., slightly smaller than that measured on the carbon magnetization. In Figure 3c, two decays are shown on a logarithmic scale. The T_1 behavior of the ^{1}H and ^{13}C nuclei is indicated by dashed lines. Separate measurements of the spin-lattice relaxation time constants give $T_1(^{1}H) = 6.1 \pm 0.3$ s and $T_1(^{13}C) = 10 \pm 1$ s in degassed $CHCl_3$; i.e., the lifetime of the LLS exceeds those of the ^{1}H and ^{13}C magnetization by factors of 7 and 4, respectively.

Figure 2c,f shows numerical simulations of the ^{13}C and ^{1}H spectra based on quantum rotor polarization of the $^{13}CH_3$ group at low temperature, giving rise to long-lived order upon dissolution, followed by slow conversion of the A/E population imbalance into magnetization components through cross-correlated heteronuclear dipole-dipole relaxation at high temperature. Although the agreement between experiment and simulation is only qualitative, it is sufficient to support the approximate validity of the model proposed here. We now sketch the components of this mechanism in more detail.

Quantum Rotor Polarization. The molecular symmetry group of the CH_3 rotor is $C_3(M)$, using the notation of Bunker and Jensen.[7] This group has three irreducible representations: A, E_a, and E_b. The Pauli principle, applied to this group, requires that the spatial A states are associated with the nuclear spin state of symmetry A, with total nuclear spin $I = {}^{3}/_{2}$. Similarly, the spatial E_a and E_b states are associated with spin states of symmetry E_b and E_a, respectively, with total nuclear spin $I = {}^{1}/_{2}$. In γ-picoline, the potential barrier for CH_3 rotation is very low (7.3 meV).[8] There is a tunneling splitting $\Delta E = 520$ μeV corresponding to $\Delta E/k_B = 6$ K between the ground spatial A state and the first excited rotational state with symmetry E_a and E_b.[8] Equilibration of the sample below ~6 K creates a large population difference between A and E, and hence between the $I = {}^{3}/_{2}$ and $I = {}^{1}/_{2}$ spin manifolds.[5b]

Dissolution. We postulate that the quantum-rotor-induced population difference between the A and E spin manifolds is substantially preserved upon the rapid warming and dissolution process. Transitions between spatial states within each manifold A and E, which are symmetry-preserving and rapid, lead to a Boltzmann distribution for the spatial states within each manifold and thus to an average spin Hamiltonian at room temperature with a greatly reduced A/E splitting.[5b] The resulting energy level diagram, with an excess population in the A state, is shown in Figure 4.

dx.doi.org/10.1021/ja410432f | J. Am. Chem. Soc. 2013, 135, 18746–18749

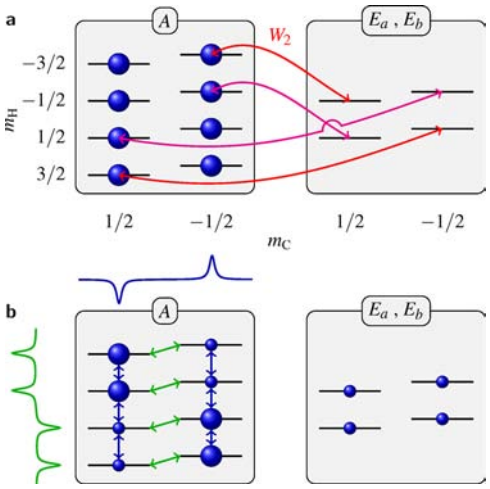

Figure 4. Energy level diagram for a $^{13}CH_3$ system. The populations immediately after dissolution from liquid helium temperature are shown as circles. For simplicity, the initial E manifolds are shown as completely depleted. Selected double-quantum ^{13}C-^{1}H cross-relaxation processes are indicated with red arrows. These processes lead to populations such as that shown in (b). Population differences within the A and E manifolds are converted into observable ^{13}C (green) and ^{1}H (blue) magnetization when a radio frequency pulse is applied, leading to the respective antiphase spectra shown on the left and top of (b).

Long-Lived Order. The relaxation properties of the $^{13}CH_3$ moiety in solution may be analyzed using Abragam−Redfield second-order perturbation theory.[9] The $^{13}CH_3$ system has been studied extensively[10] and can be modeled as a free rotor, rigidly attached to a spherical top,[11] with correlation times τ_R and τ_C for CH_3 rotation and overall tumbling, respectively. In the extreme narrowing limit, where the correlation times are much smaller than the inverse of the Larmor frequencies, the relaxation superoperator for rank-2 interactions may be written, in a static reference frame, as

$$\hat{\Gamma} = -\sum_{\lambda,\lambda'} c^{\lambda} c^{\lambda'} J_0^{\lambda,\lambda'} \sum_m (-1)^m \hat{T}_{2m}^{\lambda} \hat{T}_{2-m}^{\lambda'} \tag{1}$$

The sum is over spin interactions λ, which include the dipolar coupling for each spin pair ij, with $c^{DD,ij} = -\sqrt{6}\mu_0\gamma_i\gamma_j\hbar/(4\pi r_{ij}^3)$, and the chemical-shift anisotropy (CSA) for each spin i, with $c^{CSA,i} = \sqrt{(3/2)}\gamma_i(\sigma_{zz}^i - \sigma_{iso}^i)$. The biaxiality of the chemical shielding is ignored for simplicity. Expressions for spherical tensor operators $T_{2m}^{CSA,i}$ and $T_{2m}^{DD,ij}$ may be found in ref 11. $J_0^{\lambda,\lambda'}$ is the spectral density at zero frequency for the correlation between interactions λ and λ':

$$J_0^{\lambda,\lambda'} = \frac{1}{5} \sum_{m_1=-2}^{2} \frac{\tau_R \tau_C}{\tau_R + m_1^2 \tau_C} D_{0m_1}^2(\Omega_{PR}^{\lambda}) D_{0m_1}^{2*}(\Omega_{PR}^{\lambda'}) \tag{2}$$

where Ω_{PR}^{λ} is the set of Euler angles that describes a transformation from the principal axis system of the interaction P to a rotor frame R fixed with respect to the CH_3 group and with its z-axis aligned with the local 3-fold symmetry axis.

In the limit of rapid CH_3 rotation ($\tau_R \ll \tau_C$), the relaxation superoperator given in eq 1 has the form

$$\hat{\Gamma} = \sum_p c_p \hat{F}_p^C \hat{G}_p^C \tag{3}$$

where c_p are constants and $\hat{F}_p^C$ and $\hat{G}_p^C$ are commutation superoperators for fully symmetric operators F_p and G_p (see SI for a derivation). This form leads to vanishing transition probabilities between Hilbert-space states of different spin permutation symmetries. It corresponds to the limit of strong cross-correlation, which is associated with effects such as differential line narrowing and broadening in macromolecular systems.[10c] The dynamic symmetry expressed in eq 3 is imposed by the rapid CH_3 rotation and results in LLSs that are protected against all relaxation mechanisms internal to the CH_3 group. One such state corresponds to the difference in the mean populations of the A and E manifolds. This Liouville-space state corresponds to the Hilbert-space operator:

$$Q_{LLS} = \vec{I}_1 \cdot \vec{I}_2 + \vec{I}_1 \cdot \vec{I}_3 + \vec{I}_2 \cdot \vec{I}_3 \tag{4}$$

This operator is invariant to all nuclear spin rotations, and hence to applied magnetic fields. It is the three-spin analogue of singlet order for spin-$^1/_2$ pairs.[1f]

Cross-Relaxation. In practice, the finite correlation time τ_R leads to coupling of the LLS to population differences across the ^{1}H and ^{13}C transitions, which may be converted into observable transverse magnetization components by resonant radio frequency pulses. Finite τ_R is thus simultaneously the causes of the finite lifetime of the A/E population imbalance and of its conversion into observable magnetization; there is a compromise between the strength of the hyperpolarized signal and its lifetime.

A qualitative understanding of how the population differences develop may be obtained by considering symmetry-breaking double-quantum transitions that involve a simultaneous flip of the ^{13}C spin and of a ^{1}H spin. Figure 4 shows how such symmetry-breaking double-quantum processes lead to the observed antiphase signals for the ^{1}H spectra and also for the outer lines of the ^{13}C multiplet. However, this qualitative picture does not explain the signs of the central peaks of the ^{13}C multiplet.

An accurate representation of the relaxation processes was developed using the SpinDynamica[12] simulation platform. For example, the transition probability W_2^{AE} for symmetry-breaking double-quantum transitions caused by dipole-dipole relaxation, shown in red in Figure 4, is found to be

$$W_2^{AE} = \frac{9}{160}\tau_R (c^{DD,CH})^2 \sin^2\theta \times \frac{\tau_C(17\tau_C + 5\tau_R + 3\cos(2\theta)(5\tau_C + \tau_R))}{(\tau_C + \tau_R)(4\tau_C + \tau_R)} \tag{5}$$

where θ is the angle between a CH bond and the 3-fold symmetry axis of the CH_3 group. The transition rate W_2^{AE} indeed becomes zero in the limit of infinitely fast CH_3 rotation. The relaxation mechanisms considered in the simulations were the dipolar and CSA interactions, as well as random fields that account for additional sources of relaxation such as spin rotation and dipolar couplings with other spins. A fixed geometry was assumed, and correlation time $\tau_C \approx 5$ ps was determined from T_1 relaxation measurement of the ring carbons of γ-picoline (see SI). The rotational correlation time τ_R, the external random fields on ^{1}H and ^{13}C, and the ^{1}H and ^{13}C CSA were taken as adjustable parameters to fit the experimentally measured longitudinal relaxation rates of ^{1}H and ^{13}C and the build-up curves of the dissolution-NMR experiment. Molecular dynamics simulations and chemical-shielding simulations were used as a guide in determining the fit parameters (see SI).

The simulations shown in Figures 2 and 3 provide a qualitative description of the key features of the dissolution experiment. The relative amplitudes of the ^{13}C multiplet are in good agreement

with experiment, although the match of the simulated time courses to the experimental data is only qualitative at this stage. The inclusion of CSA is necessary to capture the spectral asymmetry. We provisionally attribute the remaining discrepancy to the role of spin-rotation relaxation, which was only included in an approximate form in the current simulation.

Polarization effects have been observed before for CH_3 groups and attributed to quantum rotor polarization.[5c] However, those effects must have a different origin than the phenomena discussed here, since they were observed in substances with small rotational splittings.

In summary, we demonstrate the existence of long-lived nuclear spin states in rapidly rotating CH_3 groups and show that this concept helps explain the strong enhancement of ^{13}C NMR signals for ^{13}C-γ-picoline upon equilibration at low temperature followed by dissolution. The curious multiplet patterns in this experiment are consistent with a relaxation model involving cross-correlated dipolar and CSA relaxation.

Two questions immediately arise: (i) Is this phenomenon expected in other substances, which exhibit higher rotational barriers than that of γ-picoline? (ii) Do other types of molecular motion allow the formation of long-lived nuclear spin states? The answer to both question is expected to be *yes*:

(i) The exceptionally low CH_3 rotational barrier in γ-picoline produces a large quantum rotor splitting and permits the generation of a substantial A/E population difference through thermal equilibration at liquid helium temperatures. However, the exceptionally low barrier is not essential for the existence of the LLS itself. Such states are indeed anticipated in the majority of substances with rapidly rotating CH_3 groups, even though only a small minority have such a low barrier as to allow polarization through thermal means. Nevertheless, for many CH_3-bearing substances, it should be possible to generate an A/E population imbalance by nuclear polarization of the proton spin system through paramagnetic doping and DNP,[2b,c] scaling as p^2, where p is the DNP-induced proton polarization. The analogous effect has been exploited in spin-$^1/_2$ pair systems to generate hyperpolarized singlet order directly by DNP.[1i]

(ii) A wide range of rapid internal molecular motions should approximately symmetrize the relaxation mechanisms. This could lead to the existence of LLSs in numerous cases where an analysis based on rigid molecular geometry would not predict their existence. Since CH_3 groups, and other mobile moieties, are ubiquitous in chemistry, this phenomenon has the potential to extend considerably the range of applicability of hyperpolarized NMR.

We expect the findings described in this paper to be only the first examples of a range of useful long-lived nuclear spin phenomena in molecular systems exhibiting rapid and symmetric internal molecular dynamics, such as flexible alkyl chains and rapidly rotating aromatic rings.

■ ASSOCIATED CONTENT

Supporting Information

Synthetic routes; experimental conditions; dissolution apparatus; details of theory and molecular dynamics. This material is available free of charge via the Internet at http://pubs.acs.org.

■ AUTHOR INFORMATION

Corresponding Author

mhl@soton.ac.uk

Notes

The authors declare no competing financial interest.

■ ACKNOWLEDGMENTS

We thank Stefan Berger and Maik Icker for sharing results and data, Walter Köckenberger and Josef Granwehr for loan of hardware, and Ole G. Johannessen and Marcel Utz for help with instrumentation. This research was supported by the Engineering and Physical Sciences Research Council (UK), by the European Research Council, and by the Wolfson Foundation.

■ REFERENCES

(1) (a) Carravetta, M.; Johannessen, O. G.; Levitt, M. H. *Phys. Rev. Lett.* **2004**, *92*, 153003. (b) Carravetta, M.; Levitt, M. H. *J. Chem. Phys.* **2005**, *122*, 214505. (c) Pileio, G.; Carravetta, M.; Levitt, M. H. *Proc. Natl. Acad. Sci. U.S.A.* **2010**, *107*, 17135. (d) Pileio, G.; Bowen, S.; Laustsen, C.; Tayler, M. C. D.; Hill-Cousins, J. T.; Brown, L. J.; Brown, R. C. D.; Ardenkjær-Larsen, J. H.; Levitt, M. H. *J. Am. Chem. Soc.* **2013**, *135*, 5084. (e) Theis, T.; Feng, Y.; Wu, T.-L.; Warren, W. S. *arXiv.orge-Print Arch., Phys.* **2013**, arXiv:1308.5666. (f) Levitt, M. H. *Annu. Rev. Phys. Chem.* **2012**, *63*, 89. (g) Grant, A. K.; Vinogradov, E. *J. Magn. Reson.* **2008**, *193*, 177. (h) Hogben, H. J.; Hore, P. J.; Kuprov, I. *J. Magn. Reson.* **2011**, *211*, 217. (i) Tayler, M. C. D.; Marco-Rius, I.; Kettunen, M. I.; Brindle, K. M.; Levitt, M. H.; Pileio, G. *J. Am. Chem. Soc.* **2012**, *134*, 7668. (j) Feng, Y.; Theis, T.; Liang, X.; Wang, Q.; Zhou, P.; Warren, W. S. *J. Am. Chem. Soc.* **2013**, *135*, 9632.

(2) (a) Ardenkjær-Larsen, J. H.; Fridlund, B.; Gram, A.; Hansson, G.; Hansson, L.; Lerche, M. H.; Servin, R.; Thaning, M.; Golman, K. *Proc. Natl. Acad. Sci. U.S.A.* **2003**, *100*, 10158. (b) Barnes, A. B.; De Paëpe, G.; van der Wel, P. C. A.; Hu, K. N.; Joo, C. G.; Bajaj, V. S.; Mak-Jurkauskas, M. L.; Sirigiri, J. R.; Herzfeld, J.; Temkin, R. J.; Griffin, R. G. *J. Low Temp. Phys.* **2008**, *34*, 237. (c) Jannin, S.; Bornet, A.; Melzi, R.; Bodenhausen, G. *Chem. Phys. Lett.* **2012**, *549*, 99.

(3) Nelson, S. J.; Kurhanewicz, J.; Vigneron, D. B.; Larson, P. E. Z.; Harzstark, A. L.; Ferrone, M.; van Criekinge, M.; Chang, J. W.; Bok, R.; Park, I.; Reed, G.; Carvajal, L.; Small, E. J.; Munster, P.; Weinberg, V. K.; Ardenkjær-Larsen, J. H.; Chen, A. P.; Hurd, R. E.; Odegardstuen, L. I.; Robb, F. J.; Tropp, J.; Murray, J. A. *Sci. Transl. Med.* **2013**, *5*, 198ra108.

(4) (a) Icker, M.; Fricke, P.; Berger, S. *J. Magn. Reson.* **2012**, *223*, 148. (b) Icker, M.; Berger, S. *J. Magn. Reson.* **2012**, *219*, 1.

(5) (a) Haupt, J. *Phys. Lett. A* **1972**, *38*, 389. (b) Horsewill, A. J. *Prog. Nucl. Magn. Reson. Spectrosc.* **1999**, *35*, 359. (c) Ludwig, C.; Saunders, M.; Marin-Montesinos, I.; Günther, U. L. *Proc. Natl. Acad. Sci. U.S.A.* **2010**, *107*, 10799. (d) Tomaselli, M.; Degen, C.; Meier, B. H. *J. Chem. Phys.* **2003**, *118*, 8559.

(6) Granwehr, J.; Leggett, J.; Köckenberger, W. *J. Magn. Reson.* **2007**, *187*, 266.

(7) Bunker, P. R.; Jensen, P. *Molecular Symmetry and Spectroscopy*, 2nd ed.; NRC Research Press: Ottawa, 2006.

(8) Prager, M.; Heidemann, A. *Chem. Rev.* **1997**, *97*, 2933.

(9) Abragam, A. *Principles of Nuclear Magnetism*; Oxford University Press, Oxford, UK, 1983.

(10) (a) Hubbard, P. S. *J. Chem. Phys.* **1970**, *52*, 563. (b) Werbelow, L. G. *J. Chem. Phys.* **1975**, *63*, 544. (c) Tugarinov, V.; Hwang, P. M.; Ollerenshaw, J. E.; Kay, L. E. *J. Am. Chem. Soc.* **2003**, *125*, 10420. (d) Müller, N.; Bodenhausen, G. *J. Chem. Phys.* **1993**, *98*, 6062.

(11) Kowalewski, J.; Mäler, L. *Nuclear Spin Relaxation in Liquids: Theory, Experiments, and Applications*; CRC Press: Boca Raton, FL, 2006.

(12) SpinDynamica, available at www.spindynamica.soton.ac.uk.

■ NOTE ADDED AFTER ASAP PUBLICATION

The magnitude of the unit for tunneling splitting given in the Quantum Rotor Polarization section was corrected on December 5, 2013.